

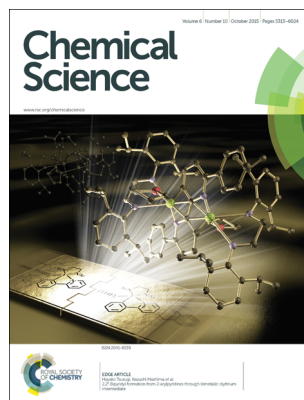
IN THIS ISSUE

ISSN 2041-6539 CODEN CSHCBM 6(10) 5313–6024 (2015)



Cover

See Dominic J. Hare, Philip A. Doble *et al.*, pp. 5383–5393. Image reproduced by permission of Dominic J. Hare from *Chem. Sci.*, 2015, 6, 5383.



Inside cover

See Hayato Tsurugi, Kazushi Mashima *et al.*, pp. 5394–5399. Image reproduced by permission of Kazushi Mashima from *Chem. Sci.*, 2015, 6, 5394.

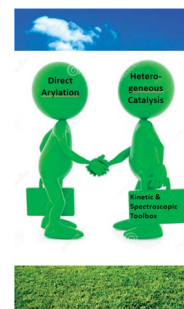
PERSPECTIVE

5338

Direct arylation and heterogeneous catalysis; ever the twain shall meet

Rafael Cano, Alexander F. Schmidt* and Gerard P. McGlacken*

We bring together the mature, yet poorly-understood, subject of heterogeneous catalysis with the rapidly expanding area of Direct Arylation, with a view towards the acceleration of catalyst design and the understanding of catalyst behaviour.



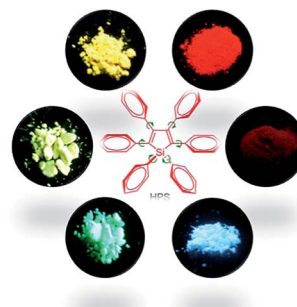
MINIREVIEWS

5347

Aggregation-induced emission of siloles

Zujin Zhao,* Bairong He and Ben Zhong Tang*

Recent advances in the structure–property relationship decipherment and luminescent functional materials development of AIE-active siloles are reviewed.



Editorial staff

Executive editor

May Copsey

Deputy editor

Jeanne Andres

Editorial production manager

Catherine Bacon

Development editor

Mina Roussanova

Publishing editors

Nelly Berg, Matthew Bown, Sage Bowser,
Hugh Cowley, Alan Holder, Samantha Ivell,
James Moore, Liisa Niitsoo, Victoria Richards,
Susan Weatherby, Rachel Wood

Publishing assistants

Natalie Ford, Bethany Johnson, Rebecca Wojturska

Publisher

Jamie Humphrey

For queries about submitted articles please contact Catherine Bacon, Editorial Production Manager, in the first instance. E-mail chemicalscience@rsc.org

For pre-submission queries please contact May Copsey, Executive Editor.

E-mail chemicalscience-rsc@rsc.org

Chemical Science (electronic: ISSN 2041-6539) is published monthly by the Royal Society of Chemistry, Thomas Graham House, Science Park, Milton Road, Cambridge, CB4 0WF, UK.

Chemical Science is a Gold Open Access journal and all articles from 2015 onwards are free to read. Please email orders@rsc.org to register your interest or contact RSC Order Department, Royal Society of Chemistry, Thomas Graham House, Science Park, Milton Road, Cambridge, CB4 0WF, UK

Tel +44 (0)1223 432398; E-mail orders@rsc.org

Advertisement sales: Tel +44 (0) 1223 432246;

Fax +44 (0) 1223 426017; E-mail advertising@rsc.org

For marketing opportunities relating to this journal, contact marketing@rsc.org

Chemical Science

www.rsc.org/chemicalscience

Editorial board

Editor-in-chief

Daniel G. Nocera, Harvard University

Associate editors

Alán Aspuru-Guzik, Harvard University
Zhenan Bao, Stanford University
Christopher C. Cummins, Massachusetts Institute of Technology
Kazunari Domen, University of Tokyo

Vy Dong, University of California, Irvine
Matthew Gaunt, University of Cambridge
Hubert Girault, Federal Polytechnic School of Lausanne
Christopher A. Hunter, University of Cambridge
David A. Leigh, University of Manchester
Kopin Liu, Academia Sinica

James K. McCusker, Michigan State University
Wonwoo Nam, Ewha Womans University
Carsten Schultz, European Molecular Biology Laboratory
F. Dean Toste, University of California, Berkeley
Haw Yang, Princeton University
Jihong Yu, Jilin University

Advisory board

Takuzo Aida, University of Tokyo
Markus Antonietti, Max Planck Institute of Colloids and Interfaces
Polly Arnold, University of Edinburgh
Xinhe Bao, Dalian Institute of Chemical Physics
Guy Bertrand, University of California, Los Angeles
Jeffrey Bode, Swiss Federal Institute of Technology Zurich
Christopher Chang, University of California, Berkeley
Chi-Ming Che, University of Hong Kong
Jason Chin, Medical Research Council Laboratory of Molecular Biology
Daniel Chiu, University of Washington
Graham Cooks, Purdue University
Eugenio Coronado, University of Valencia
Lee Cronin, University of Glasgow
James Durrant, Imperial College London
Ben Feringa, University of Groningen
Cynthia Friend, Harvard University
Makoto Fujita, University of Tokyo
Philip Gale, University of Southampton
Song Gao, Peking University
Jinlong Gong, Tianjin University
Justin Gooding, University of New South Wales
Michael Graetzel, Federal Polytechnic School of Lausanne
Duncan Graham, University of Strathclyde
Buxing Han, Chinese Academy of Sciences
Jeremy Harvey, University of Bristol

Christy Haynes, University of Minnesota
Johan Hofkens, Catholic University of Leuven
Linda Hsieh-Wilson, California Institute of Technology
Eric Jacobsen, Harvard University
Takashi Kato, University of Tokyo
Seong Keun Kim, Seoul National University
Jerome Lacour, University of Geneva
James Leighton, Columbia University
Steve Ley, University of Cambridge
Chao-Jun Li, McGill University
Wenbin Lin, University of North Carolina
Watson Loh, Instituto de Química
Julie Macpherson, University of Warwick
Stephen Mann, University of Bristol
Bert Meijer, Eindhoven University of Technology
Nils Metzler-Nolte, Ruhr University Bochum
Scott Miller, Yale University
Daniel Mindiola, Indiana University
Mohammad Movassaghi, Massachusetts Institute of Technology
Jonathan Nitschke, University of Cambridge
Kyoko Nozaki, University of Tokyo
Takashi Ooi, Nagoya University
Rachel O'Reilly, University of Warwick
Michel Orrit, Leiden University
Oleg Ozerov, Texas A&M University
Hongkun Park, Harvard University

Rasmita Raval, University of Liverpool
Paul Reider, Princeton University
Stuart Rowan, Case Western Reserve University
Richmond Sarpong, University of California, Berkeley
Gregory Scholes, University of Toronto
Oliver Seitz, Humboldt University of Berlin
Kay Severin, Federal Polytechnic School of Lausanne
Mikiko Sodeoka, RIKEN
Brian Stoltz, California Institute of Technology
Weihong Tan, University of Florida
He Tian, East China University of Science and Technology
Zhong-Qun Tian, Xiamen University
Andrei Tokmakoff, University of Chicago
Jan Van Hest, Radboud University
Tom Welton, Imperial College London
Christina White, University of Illinois
Martin Wolf, Fritz Haber Institute of the Max Planck Society
Omar Yaghi, University of California, Los Angeles
Vivian Yam, University of Hong Kong
Yang Yang, University of California, Los Angeles
Shu-Hong Yu, University of Science and Technology of China
Qi-Lin Zhou, Nankai University

Information for authors

Full details on how to submit material for publication in Chemical Science are given in the Instructions for Authors (available from <http://www.rsc.org/authors>). Submissions should be made via the journal's homepage: <http://www.rsc.org/chemicalscience>.

Authors may reproduce/republish portions of their published contribution without seeking permission from the RSC, provided that any such republication is accompanied by an acknowledgement in the form: (Original Citation) – Reproduced by permission of The Royal Society of Chemistry.

This journal is ©The Royal Society of Chemistry 2015. Apart from fair dealing for the purposes of research or private study for non-commercial purposes, or criticism or review, as permitted under the Copyright, Designs and

Patents Act 1988 and the Copyright and Related Rights Regulation 2003, this publication may only be reproduced, stored or transmitted, in any form or by any means, with the prior permission in writing of the Publishers or in the case of reprographic reproduction in accordance with the terms of licences issued by the Copyright Licensing Agency in the UK. US copyright law is applicable to users in the USA.

The Royal Society of Chemistry takes reasonable care in the preparation of this publication but does not accept liability for the consequences of any errors or omissions.

© The paper used in this publication meets the requirements of ANSI/NISO Z39.48–1992 (Permanence of Paper).

Registered Charity No. 207890.



5366

Guillaume Duret, Robert Quinlan, Philippe Bisseret*
and Nicolas Blanchard*

Reaction scheme for the synthesis of Bodipy dyes:

- Left Pathway:**
 - Starting material: $\text{R}-\text{BF}_3\text{K}^+$ (with a dimethylaminomethyl group)
 - Reaction: $\xrightarrow{\text{visible light}}$
 - Intermediate: $\text{L}-\text{BH}_2^{\bullet-}$
 - Reaction: $\xrightarrow{\text{Barton deoxygenation}}$
 - Products:
 - C-C, B-S bond formation
 - C-X bond reduction
 - Barton deoxygenation
- Middle Pathway:**
 - Starting material: $\text{R}-\text{B}(\text{OR})_2$ (cyclic boronate ester)
 - Reaction: $\xrightarrow{\text{visible light}}$
 - Intermediate: R^\bullet
 - Reaction: $\xrightarrow{\text{dual catalysis}}$
 - Products:
 - C-O bond formation
 - C-C (alkyl, alkenyl, alkynyl, benzyl) bond formation
 - dual catalysis
- Right Pathway:**
 - Starting material: $\text{R}-\text{B}(\text{OR})_2$ (fluorinated boronate ester)
 - Reaction: $\xrightarrow{\text{visible light}}$
 - Intermediate: Bodipy^*
 - Reaction: $\xrightarrow{\text{uncoupling of biomolecules}}$
 - Products:
 - oxidation of sulfides
 - oxidation of naphthal
 - arylation of heteroaromatics
 - cationic polymerisation
 - uncoupling of biomolecules

5383

Bence Paul, Dominic J. Hare,* David P. Bishop,
Chad Paton, Van Tran Nguyen, Nerida Cole,
Megan M. Niedwiecki, Erica Andreozzi, Angela Vais,
Jessica L. Billings, Lisa Bray, Ashley I. Bush, Gawain McColl,
Blaine R. Roberts, Paul A. Adlard, David I. Finkelstein,
John Hellstrom, Janet M. Hergt, Jon D. Woodhead
and Philip A. Doble*

5394

[illegible]

Formation of dianionic 2,2'-bipyridyl-bridged dinuclear yttrium complexes proceeded upon treatment of $(\text{ArNCH}_2\text{CH}_2\text{NAr})\text{Y}(\text{CH}_2\text{SiMe}_3)(\text{THF})_2$ with 2-arylpyridine, in which mononuclear (2-pyridylphenyl)yttrium complexes were detected as key intermediates).

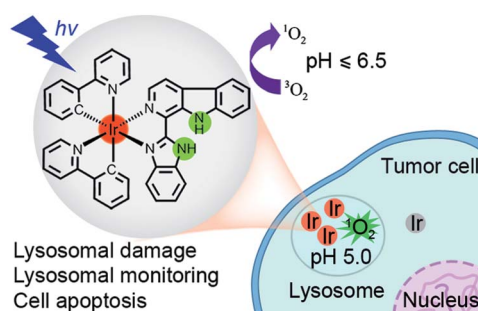
5400

Figure 10 is a line graph showing tumor growth curves for vehicle control and 100 mg/kg of 1a. The y-axis represents Tumor volume (mm³) from 0 to 2500, and the x-axis represents Days from 0 to 20. The vehicle control group (circles) shows a steady increase in tumor volume, reaching approximately 1450 mm³ by day 16. The 100 mg/kg of 1a group (squares) shows significantly lower tumor growth, reaching approximately 800 mm³ by day 16. A significant difference is marked by ** at day 16. An inset shows the chemical structure of the 1a complex, featuring a bis-imidazole ligand coordinated to a central metal atom, with OTf⁻ counterions.

Days	Vehicle control (mm ³)	100 mg/kg of 1a (mm ³)
0	~100	~100
2	~150	~150
4	~250	~200
6	~350	~250
8	~450	~300
10	~600	~400
12	~850	~500
14	~1050	~750
16	~1450	~800

This is the first report of a metal complex that targets the BRD4-acylated histone protein-protein interaction (PPI).

5409

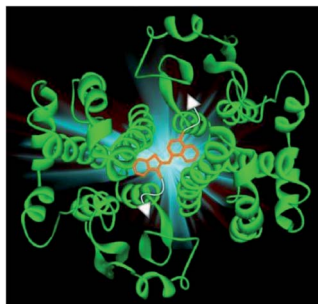


Cyclometalated iridium(III) complexes as lysosome-targeted photodynamic anticancer and real-time tracking agents

Liang He, Yi Li, Cai-Ping Tan,* Rui-Rong Ye, Mu-He Chen, Jian-Jun Cao, Liang-Nian Ji and Zong-Wan Mao*

We report the rational design and photodynamic anticancer mechanism studies of iridium(III) complexes with pH-responsive singlet oxygen ($^1\text{O}_2$) production and lysosome-specific imaging properties.

5419

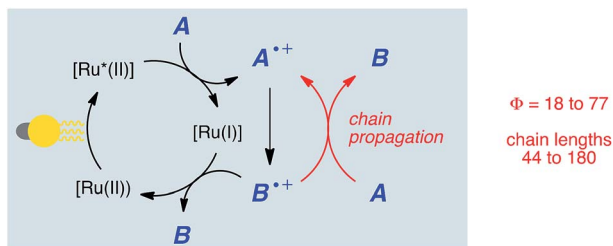


Protein recognition by bivalent, 'turn-on' fluorescent molecular probes

Linor Unger-Angel, Bhimsen Rout, Tal Ilani, Miriam Eisenstein, Leila Motiei and David Margulies*

The selective and sensitive identification of different proteins becomes possible by modifying the known intercalating dye, thiazole orange, with two protein binders. These 'turn-on' fluorescence probes enable the identification of acetylcholinesterase, glutathione-S-transferases and avidin with high affinity, specificity, and high signal-to-noise ratio.

5426

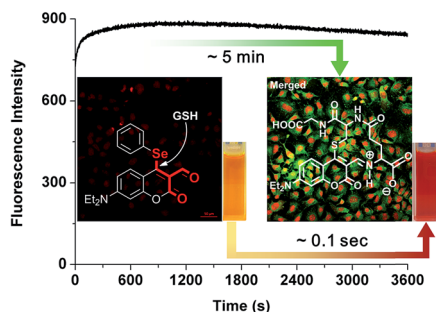


Characterizing chain processes in visible light photoredox catalysis

Megan A. Cismesia and Tehshik P. Yoon*

The combination of quantum yield and luminescence quenching measurements provides a method to rapidly characterize the occurrence of chain processes in a variety of photoredox reactions.

5435



Exceptional time response, stability and selectivity in doubly-activated phenyl selenium-based glutathione-selective platform

Youngsam Kim, Sandip V. Mulay, Minsuk Choi, Seungyeon B. Yu, Sangyong Jon and David G. Churchill*

Outstanding glutathione chemosensing selectivity with a new coumarin-based probe is reported and discussed in the context of live cell experiments; the point of attack is flanked by two proximal carbonyl groups.

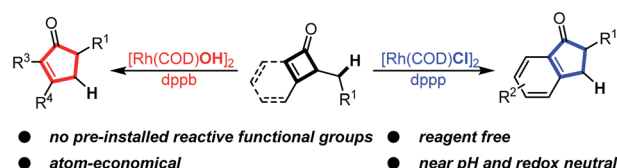


5440

Rh-catalyzed reagent-free ring expansion of cyclobutenones and benzocyclobutenones

Peng-hao Chen, Joshua Sieber, Chris H. Senanayake and Guangbin Dong*

A reagent-free Rh-catalyzed ring-expansion reaction via C–C cleavage of cyclobutenones and benzocyclobutenones is reported.

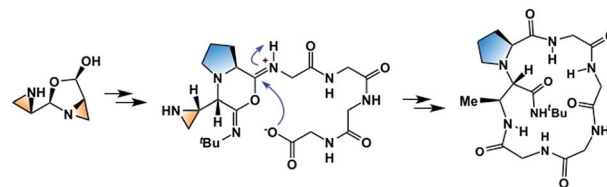


5446

Mechanistic investigation of aziridine aldehyde-driven peptide macrocyclization: the imidoanhydride pathway

Serge Zaretsky, Jennifer L. Hickey, Joanne Tan, Dmitry Pichugin, Megan A. St. Denis, Spencer Ler, Benjamin K. W. Chung, Conor C. G. Scully and Andrei K. Yudin*

Aziridine aldehydes participate in a multicomponent reaction with α -amino amides and isocyanides to generate reactive imidoanhydride intermediates.

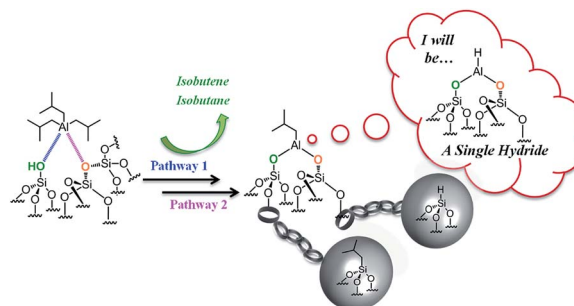


5456

Well-defined silica supported aluminum hydride: another step towards the utopian single site dream?

Baraa Werghi, Anissa Bendjeriou-Sedjerari, Julien Sofack-Kreutzer, Abdesslem Jedidi, Edy Abou-Hamad, Luigi Cavallo* and Jean-Marie Basset*

Reaction of triisobutylaluminum with SBA15₇₀₀ at room temperature occurs by two parallel pathways involving either silanol or siloxane bridges.

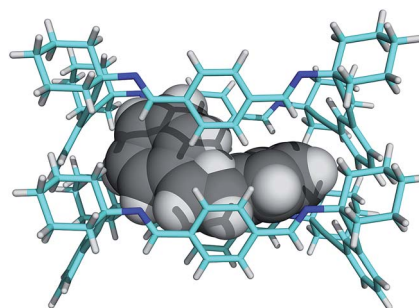


5466

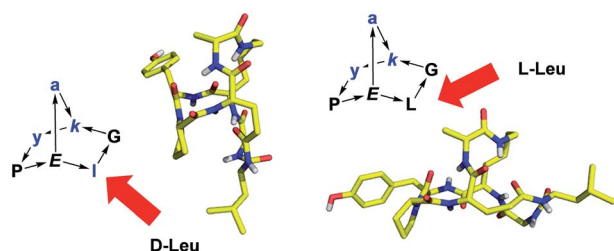
A crystalline sponge based on dispersive forces suitable for X-ray structure determination of included molecular guests

Elena Sanna, Eduardo C. Escudero-Adán, Antonio Bauzá, Pablo Ballester, Antonio Frontera, Carmen Rotger and Antonio Costa*

A new organic material assembled by dispersive forces exhibits stable one-dimensional channels suitable as the solid support in X-ray structural studies by the crystalline sponge method.



5473

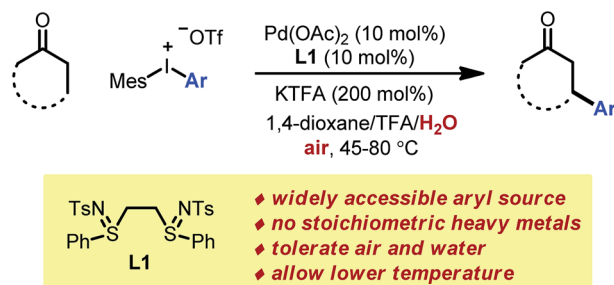


Bridged bicyclic peptides as potential drug scaffolds: synthesis, structure, protein binding and stability

Marco Bartoloni, Xian Jin, Maria José Marcaida, João Banha, Ivan Dibonaventura, Swathi Bongoni, Kathrin Bartho, Olivia Gräbner, Michael Sefkow, Tamis Darbre and Jean-Louis Reymond*

Diastereomeric norbornapeptides represent globular scaffolds with geometries determined by the chirality of amino acid residues and sharing structural features of β -turns and α -helices.

5491

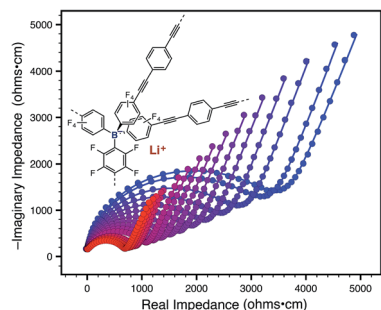


Palladium-catalyzed direct β -arylation of ketones with diaryliodonium salts: a stoichiometric heavy metal-free and user-friendly approach

Zhongxing Huang, Quynh P. Sam and Guangbin Dong*

A user-friendly protocol for the Pd-catalyzed direct β -arylation of ketones is described, which avoids the use of stoichiometric heavy metals.

5499

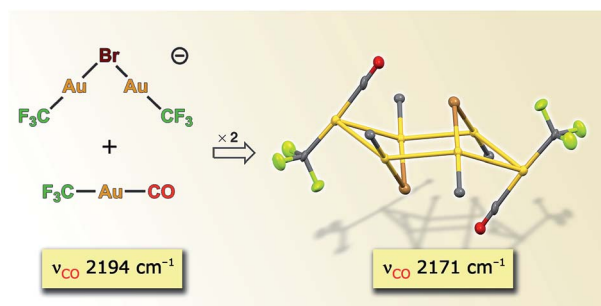


Tetraarylborate polymer networks as single-ion conducting solid electrolytes

Jeffrey F. Van Humbeck, Michael L. Aubrey, Alaaeddin Alsbaiee, Rob Ameloot, Geoffrey W. Coates, William R. Dichtel and Jeffrey R. Long*

A new family of solid polymer electrolytes based upon anionic tetrakis(phenyl)borate tetrahedral nodes and linear bis-alkyne linkers is reported.

5506



A hexanuclear gold carbonyl cluster

Sonia Martínez-Salvador, Larry R. Falvello, Antonio Martín and Babil Menjón*

Aurophilic interactions are responsible for the spontaneous formation of a cyclo-Au_6 carbonyl cluster whereby significant ν_{CO} lowering is observed.

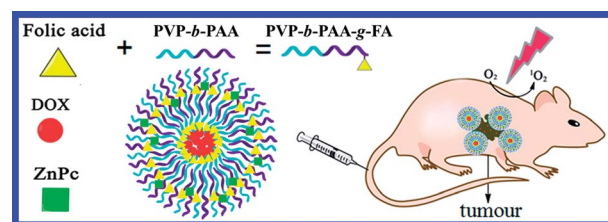


5511

A supramolecular nanovehicle toward systematic, targeted cancer and tumor therapy

Ruizheng Liang, Shusen You, Lina Ma, Chunyang Li, Rui Tian, Min Wei,* Dan Yan,* Meizhen Yin,* Wantai Yang, David G. Evans and Xue Duan

A supramolecular nanovehicle (denoted as SNV) was fabricated by encapsulating zinc phthalocyanine (ZnPc) and doxorubicin (DOX) into a copolymer (PVP-*b*-PAA-*g*-FA), so as to achieve systematic and targeted tumor imaging and therapy.

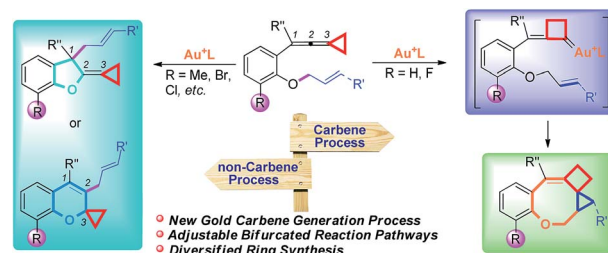


5519

Gold(I)-catalyzed cycloisomerization of vinylidenecyclopropane-enes via carbene or non-carbene processes

De-Yao Li, Yin Wei, Ilan Marek, Xiang-Ying Tang* and Min Shi*

Gold catalyzed cycloisomerization of aromatic ring tethered vinylidenecyclopropane-enes provides a divergent synthetic protocol for the construction of O-containing fused heterocycles through controllable carbene or non-carbene related processes.

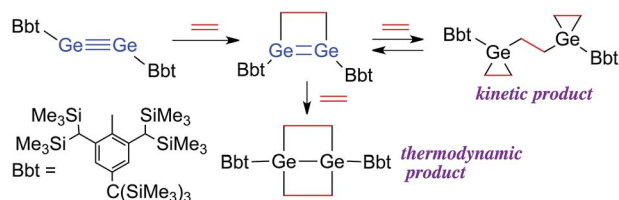


5526

Reaction of a diaryldigermene with ethylene

Takahiro Sasamori,* Tomohiro Sugahara, Tomohiro Agou, Koh Sugamata, Jing-Dong Guo, Shigeru Nagase and Norihiro Tokitoh*

Reaction of a stable digermene with ethylene afforded the corresponding 1,2-digermacyclobutene. Depending on the reaction conditions applied, further reaction of this 1,2-digermacyclobutene with ethylene furnished two different reaction products: a 1,4-digerma-bicyclo[2.2.0]hexane or a bis(germiranyl)ethane.

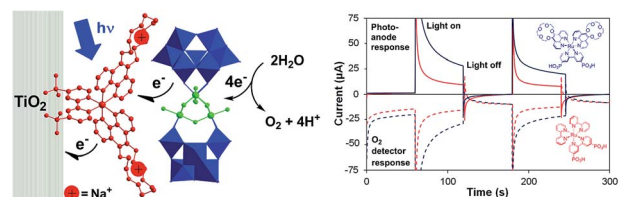


5531

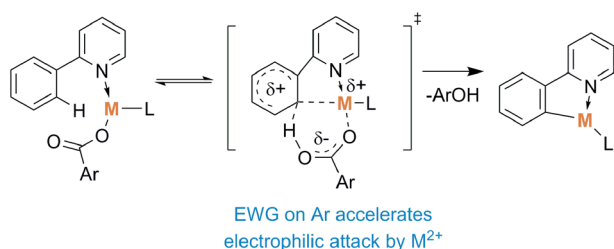
Water splitting with polyoxometalate-treated photoanodes: enhancing performance through sensitizer design

John Fielden,* Jordan M. Sumliner, Nannan Han, Yurii V. Geletii, Xu Xiang, Djamaladdin G. Musaev,* Tianquan Lian* and Craig L. Hill*

Improved sensitizer design dramatically enhances visible light-driven water oxidation from dye-sensitized TiO₂ photoanodes treated with polyoxometalate water oxidation catalyst [{Ru₄O₄(OH)₂(H₂O)₄}(γ-SiW₁₀O₃₆)₂]¹⁰⁻.



5544

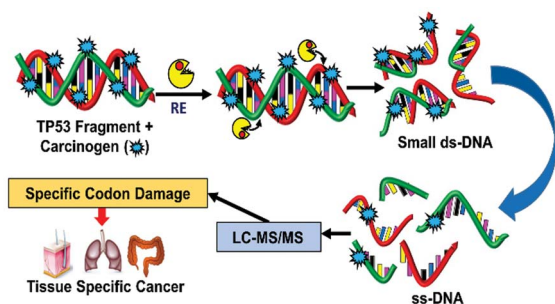


Carboxylate-assisted C–H activation of phenylpyridines with copper, palladium and ruthenium: a mass spectrometry and DFT study

A. Gray, A. Tsybizova and J. Roithova*

The transition state of metal carboxylate mediated C–H activation is associated with carbon–metal bond formation supported by electron-poor carboxylates.

5554

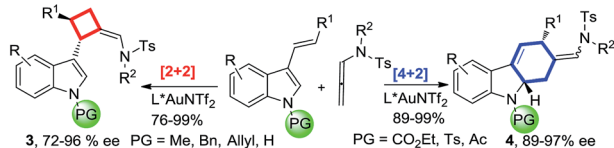


Chemical selectivity of nucleobase adduction relative to *in vivo* mutation sites on exon 7 fragment of p53 tumor suppressor gene

Spundana Malla, Kartteek Kadimisetty, You-Jun Fu, Dharamainder Choudhary, Ingela Jansson, John B. Schenkman and James F. Rusling*

A 32-bp fragment of P53 gene reacted with benzo[a]pyrene metabolite BPDE was analyzed by LC-MS/MS. Chemically reactive sites were similar to frequently mutated codons in tumors.

5564

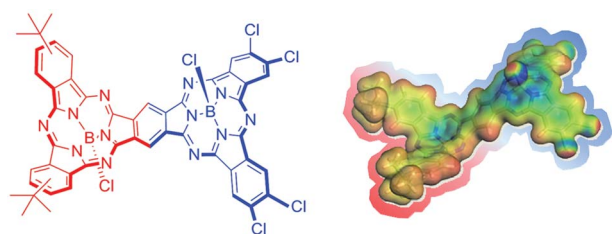


Enantioselective gold-catalyzed intermolecular [2+2] versus [4+2]-cycloadditions of 3-styrylindoles with *N*-allenamides: observation of interesting substituent effects

Yidong Wang, Peichao Zhang, Yuan Liu, Fei Xia* and Junliang Zhang*

The cycloaddition mode ([2+2] vs. [4+2]) can be unexpectedly switched by the simple modification of the *N*-substituent of the 3-styrylindoles.

5571



A push–pull unsymmetrical subphthalocyanine dimer

Germán Zango, Johannes Zirzmeier, Christian G. Claessens, Timothy Clark*, M. Victoria Martínez-Díaz*, Dirk M. Guldi* and Tomás Torres*

Unsymmetrical subphthalocyanine fused dimers have been prepared, resulting in unprecedented push–pull π -extended curved aromatic macrocycles.

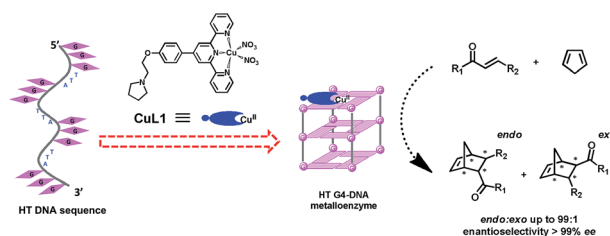


5578

Terpyridine–Cu(II) targeting human telomeric DNA to produce highly stereospecific G-quadruplex DNA metalloenzyme

Yinghao Li, Mingpan Cheng, Jingya Hao, Changhao Wang, Guoqing Jia* and Can Li*

A highly stereospecific G-quadruplex DNA metalloenzyme was found by exploring the G-quadruplex targeting ligand pool.

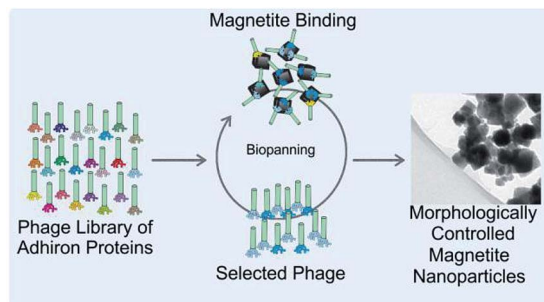


5586

Phage display selected magnetite interacting Adhirons for shape controlled nanoparticle synthesis

Andrea E. Rawlings, Jonathan P. Bramble, Anna A. S. Tang, Lori A. Somner, Amy E. Monnington, David J. Cooke, Michael J. McPherson, Darren C. Tomlinson and Sarah S. Staniland*

Biopanning was used to generate novel artificial binding proteins which are able to control the formation of synthetic cubic nanoparticles of magnetite.

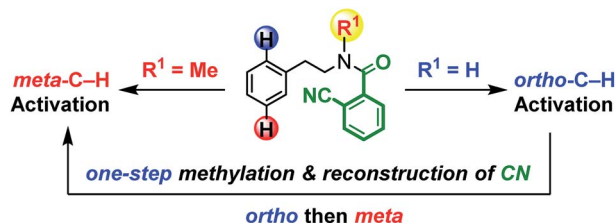


5595

Pd(II)-catalyzed remote regiodivergent *ortho*- and *meta*-C–H functionalizations of phenylethylamines

Shangda Li, Huafang Ji, Lei Cai and Gang Li*

A methylation switches the remote regioselectivity of C–H functionalizations of phenylethylamines.

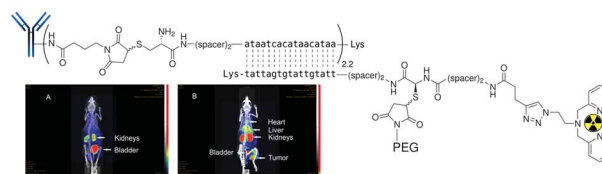


5601

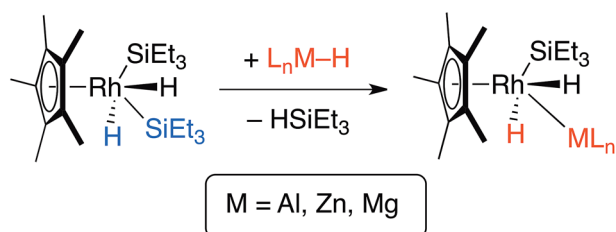
In vivo demonstration of an active tumor pretargeting approach with peptide nucleic acid bioconjugates as complementary system

Anna Leonidova, Christian Foerster, Kristof Zarschler, Maik Schubert, Hans-Jürgen Pietzsch, Jörg Steinbach, Ralf Bergmann, Nils Metzler-Nolte, Holger Stephan* and Gilles Gasser*

The first successful application of a pretargeting approach using a PNA-modified epidermal growth factor receptor specific antibody and a complementary ^{99m}Tc-labeled PNA is presented.



5617

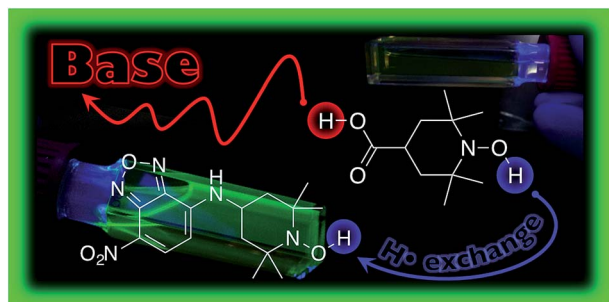


Addition of aluminium, zinc and magnesium hydrides to rhodium(III)

Olga Ekkert, Andrew J. P. White, Harold Toms and Mark R. Crimmin*

We report the addition of M–H bonds (M = Al, Zn, Mg) to a Rh(III) intermediate generated from the reductive elimination of triethylsilane from $[\text{Cp}^*\text{Rh}(\text{H})_2(\text{SiEt}_3)_2]$.

5623

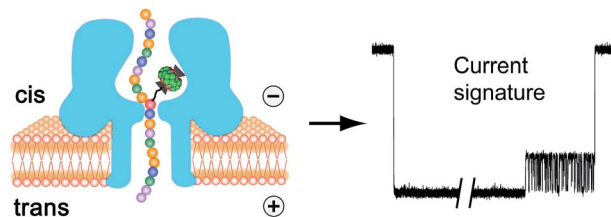


Experimental demonstration of pH-dependent electrostatic catalysis of radical reactions

Marta Klinska, Leesa M. Smith, Ganna Gryn'ova, Martin G. Banwell and Michelle L. Coote*

Fluorescence spectroscopy demonstrated pH-dependent electrostatic effects on the kinetics and thermodynamics of hydrogen atom transfer between 1-hydroxy-2,2,6,6-tetramethyl-4-piperidinecarboxylic acid and {2,2,6,6-tetramethyl-4-[(7-nitro-2,1,3-benzoxadiazol-4-yl)amino]-1-piperidinyloxydanyl radical in dichloromethane.

5628

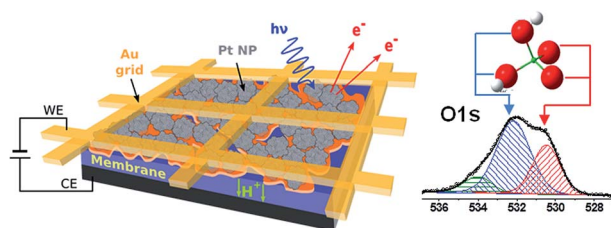


Detection of 5-methylcytosine and 5-hydroxymethylcytosine in DNA via host-guest interactions inside α -hemolysin nanopores

Tao Zeng, Lei Liu, Ting Li, Yuru Li, Juan Gao, Yuliang Zhao* and Hai-Chen Wu*

After selective modification with a host-guest complex, 5-methylcytosine and 5-hydroxymethylcytosine in ssDNA can be unambiguously detected by the generation of characteristic current events during the translocation of the modified DNA through α -hemolysin nanopores.

5635



In situ investigation of dissociation and migration phenomena at the Pt/electrolyte interface of an electrochemical cell

Yeuk Ting Law, Spyridon Zafeiratos, Stylianos G. Neophytides, Alin Orfanidi, Dominique Costa, Thierry Dintzer, Rosa Arrigo, Axel Knop-Gericke, Robert Schlögl and Elena R. Savinova*

Using near ambient pressure X-ray photoelectron spectroscopy we probe *in situ* the double layer at the Pt/liquid electrolyte interface.

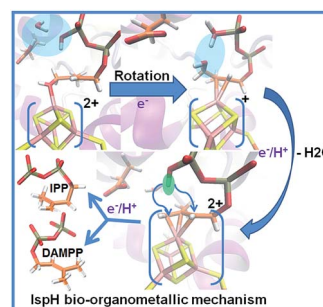


5643

Mechanistic insights into the reductive dehydroxylation pathway for the biosynthesis of isoprenoids promoted by the IspH enzyme

Safwat Abdel-Azeim, Abdesslem Jedidi, Jorg Eppinger and Luigi Cavallo*

We report an integrated QM/MM study of the bio-organometallic reaction pathway of the reductive dehydroxylation of (*E*)-4-hydroxy-3-methylbut-2-enyl pyrophosphate (HMBPP).

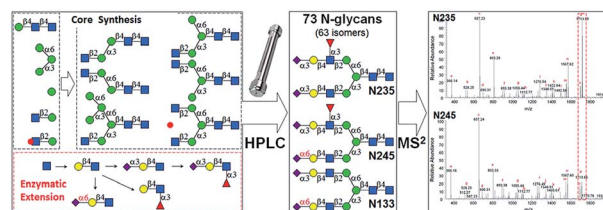


5652

Efficient chemoenzymatic synthesis of an N-glycan isomer library

Lei Li, Yunpeng Liu, Cheng Ma, Jingyao Qu, Angie D. Calderon, Baolin Wu, Na Wei, Xuan Wang, Yuxi Guo, Zhongying Xiao, Jing Song, Go Sugiarto, Yanhong Li, Hai Yu, Xi Chen and Peng George Wang*

An efficient chemoenzymatic synthesis strategy and a HILIC-based purification approach enabled rapid access to an N-glycan isomer library.

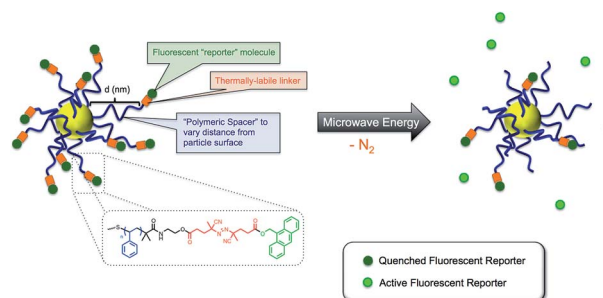


5662

Probing the surface-localized hyperthermia of gold nanoparticles in a microwave field using polymeric thermometers

Christopher P. Kabb, R. Nicholas Carmean and Brent S. Sumerlin*

Gold nanoparticles decorated with "polymeric thermometers," consisting of a polymeric spacer, thermally-labile azo linker, and fluorescent tag, were used to quantify the extent of localized hyperthermia under microwave irradiation.

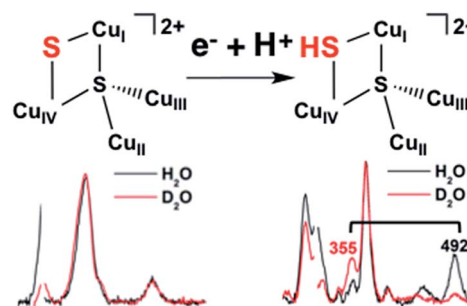


5670

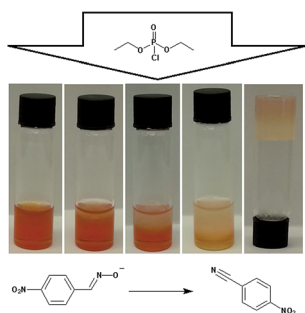
Protonation state of the Cu₄S₂ Cu_z site in nitrous oxide reductase: redox dependence and insight into reactivity

Esther M. Johnston, Simone Dell'Acqua, Sofia R. Pauleta, Isabel Moura and Edward I. Solomon*

The edge ligand in the Cu₄S₂ Cu_z form of nitrous oxide reductase is a μ₂-thiolate in the 1-hole and a μ₂-sulfide in the 2-hole redox state, leading to proton-coupled electron transfer reactivity.



5680

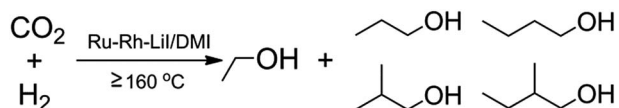


Detection and remediation of organophosphorus compounds by oximate containing organogels

Jennifer R. Hiscock, Mark R. Sambrook, Neil J. Wells and Philip A. Gale*

A series of supramolecular diamide organogels containing a reactive compound for the remediation of organophosphorus (OP) species, in particular OP chemical warfare agents (CWAs), has been prepared in DMSO.

5685

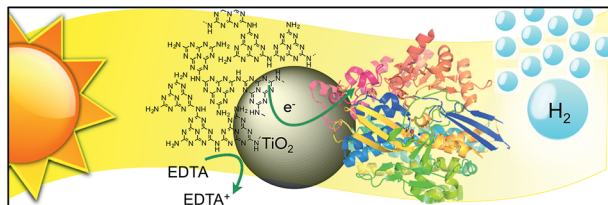


Highly selective hydrogenation of CO₂ into C₂₊ alcohols by homogeneous catalysis

Qingli Qian,* Meng Cui, Zhenhong He, Congyi Wu, Qinggong Zhu, Zhaofu Zhang, Jun Ma, Guanying Yang, Jingjing Zhang and Buxing Han*

Methanol, ethanol, propanol, 2-methyl propanol, butanol, and 2-methyl butanol were produced in homogeneous CO₂ hydrogenation with a selectivity for C₂₊ alcohols of 96.4%.

5690

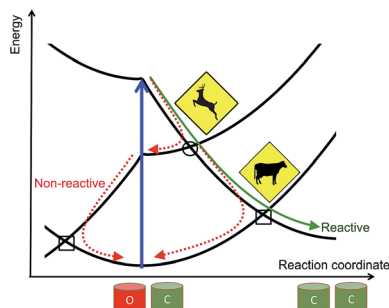


Carbon nitride–TiO₂ hybrid modified with hydrogenase for visible light driven hydrogen production

Christine A. Caputo, Lidong Wang, Radim Beranek and Erwin Reisner*

Solar light driven hydrogen production with a heterogenised hydrogenase on a carbon nitride–TiO₂ hybrid is reported that sets a new benchmark for photo-H₂ production.

5695



A curve-crossing model to rationalize and optimize diarylethene dyads

Benjamin Lasorne,* Arnaud Fihey, David Mende-Tapia and Denis Jacquemin*

Extra crossing points play a key role in the photochemistry of diarylethene dyads.

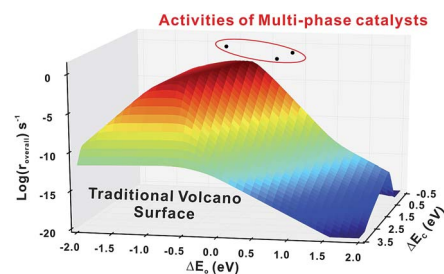


5703

Possibility of designing catalysts beyond the traditional volcano curve: a theoretical framework for multi-phase surfaces

Ziyun Wang, Hai-Feng Wang and P. Hu*

The current theory of catalyst activity in heterogeneous catalysis is mainly obtained from the study of catalysts with mono-phases, while most catalysts in real systems consist of multi-phases, the understanding of which is far short of chemists' expectation.



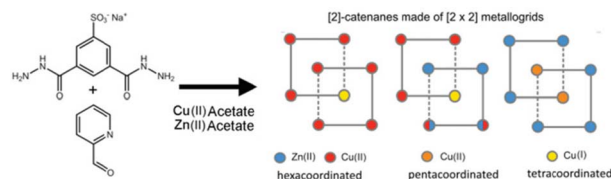
Multi-phase catalysts VS. Mono-phase catalysts

5712

Mixed valence mono- and hetero-metallic grid catenanes

Chandan Giri, Filip Topić, Massimo Cametti* and Kari Rissanen*

Multicomponent self-assembly was employed to obtain, in the solid state, a series of mixed valence mono- and hetero-metallic grid catenanes, which were characterized by single crystal X-ray diffraction.

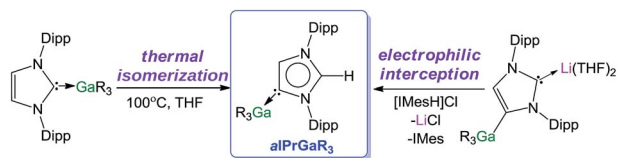


5719

Rational synthesis of normal, abnormal and anionic NHC–gallium alkyl complexes: structural, stability and isomerization insights

Marina Uzelac, Alberto Hernán-Gómez, David R. Armstrong, Alan R. Kennedy and Eva Hevia*

Using two alternative methodologies, new light has been shed on the stability and rational formation of abnormal NHC–gallium complexes.

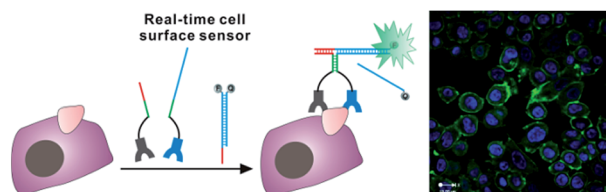


5729

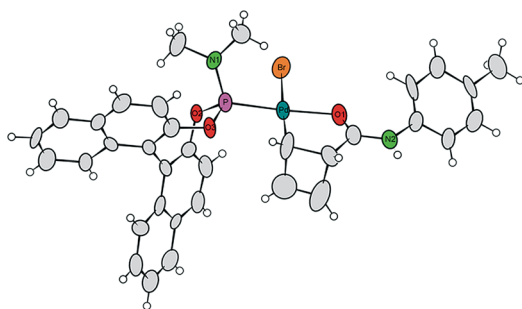
Constructing real-time, wash-free, and reiterative sensors for cell surface proteins using binding-induced dynamic DNA assembly

Yanan Tang, Zhixin Wang, Xiaolong Yang, Junbo Chen, Linan Liu, Weian Zhao, X. Chris Le and Feng Li*

A real-time, wash-free, and reiterative sensor is constructed for monitoring cell surface proteins using the principle of binding-induced DNA dynamic assembly.



5734

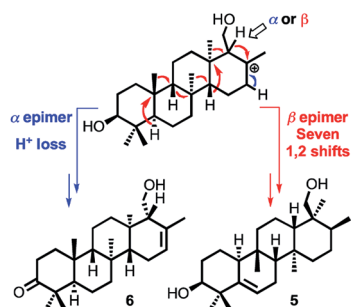


Dynamic behaviour of monohaptoallylpalladium species: internal coordination as a driving force in allylic alkylation chemistry

Lan-Gui Xie, Viktor Bagutski, Davide Audisio, Larry M. Wolf, Volker Schmidts, Kathrin Hofmann, Cornelia Wirtz, Walter Thiel, Christina M. Thiele* and Nuno Maulide*

Structural and reactivity studies of internally coordinated monohaptoallylpalladium(II) complexes.

5740

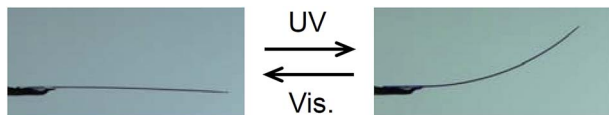


Biosynthetic insights provided by unusual sesterterpenes from the medicinal herb *Aletris farinosa*

Victoria L. Challinor, Ryne C. Johnston, Paul V. Bernhardt, Reginald P. Lehmann, Elizabeth H. Krenske and James J. De Voss*

Configuration of a single stereocenter determines if a key carbocation in sesterterpene biosynthesis undergoes simple elimination or a cascade of seven 1,2-methyl and hydride migrations.

5746

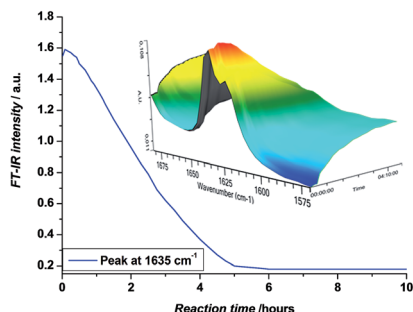


Light-driven bending of diarylethene mixed crystals

Satoko Ohshima, Masakazu Morimoto and Masahiro Irie*

The bending response of mixed crystals by selective photoisomerization revealed that the local shape change of each molecule is additively linked to the macroscopic deformation of the crystals.

5753



Synthesis of sequence-defined acrylate oligomers via photo-induced copper-mediated radical monomer insertions

Joke Vandenberg, Gunter Reekmans, Peter Adriaensens and Tanja Junkers*

Photo-induced copper-mediated radical polymerization is used to synthesize monodisperse sequence defined acrylate oligomers via consecutive single unit monomer insertion reactions and intermediate purification of the compounds by column or preparative recycling size exclusion chromatography.

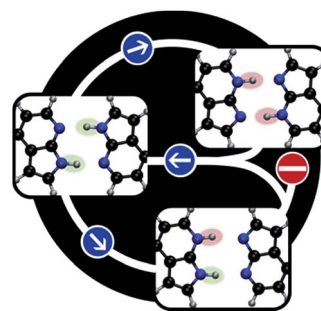


5762

Stepwise double excited-state proton transfer is not possible in 7-azaindole dimer

Rachel Crespo-Otero,^{*} Nawee Kungwan^{*}
and Mario Barbatti^{*}

Topographical analysis of the dimer's excited state shows that internal conversion after first proton transfer blocks the stepwise process.

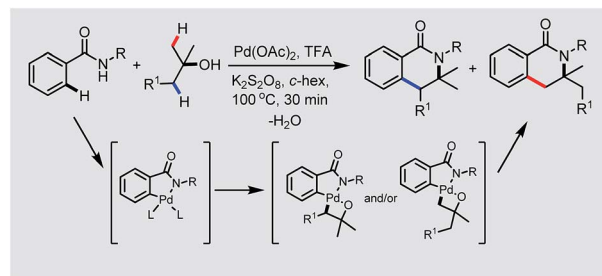


5768

Modular synthesis of dihydro-isoquinolines: palladium-catalyzed sequential C(sp²)-H and C(sp³)-H bond activation

Weidong Liu, Qingzhen Yu, Le'an Hu, Zenghua Chen
and Jianhui Huang^{*}

An efficient synthesis of dihydro-isoquinolines *via* a Pd-catalyzed double C-H bond activation/annulation featuring a short reaction time, high atom economy and the formation of a sterically less favoured tertiary C-N bond.

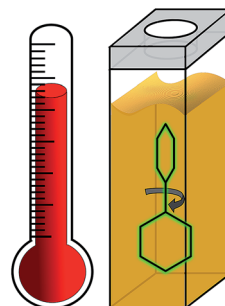


5773

Unravelling the effect of temperature on viscosity-sensitive fluorescent molecular rotors

Aurimas Vyšniauskas, Maryam Qurashi, Nathaniel Gallop,
Milan Balaz, Harry L. Anderson and Marina K. Kuimova^{*}

We examine the effect of temperature on three viscosity-sensitive fluorophores termed 'molecular rotors'. In the case of the conjugated porphyrin dimer, it can be used for measuring both viscosity and temperature concurrently.



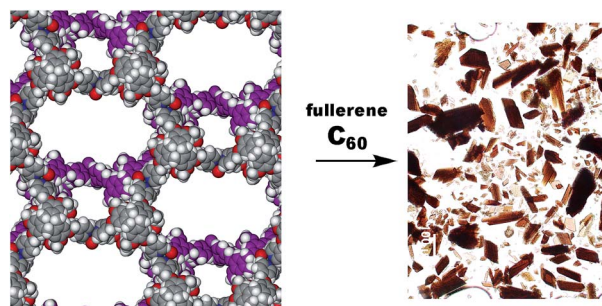
Molecular sensors	η	T
BODIPY	✓	✗
Kiton Red	✓ or ✗	✗ ✓
Porphyrin dimer	✓	✓

5779

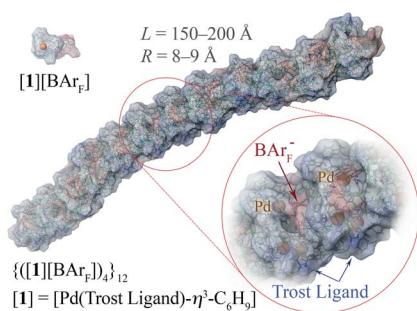
Copper coordination polymers from cavitand ligands: hierarchical spaces from cage and capsule motifs, and other topologies

Flora L. Thorp-Greenwood, Tanya K. Ronson
and Michael J. Hardie^{*}

Copper coordination polymers from cavitand ligands are reported including networked cage-motif structures, one of which takes up C₆₀ from solution.



5793

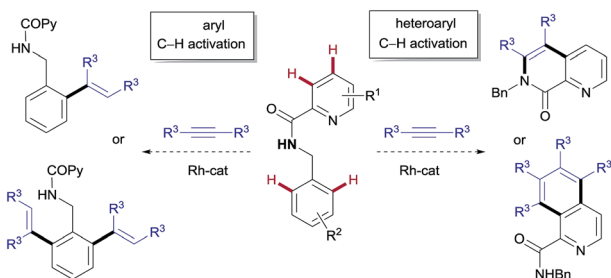


Pd- $\eta^3\text{-C}_6\text{H}_9$ complexes of the Trost modular ligand: high nuclearity columnar aggregation controlled by concentration, solvent and counterion

Daugirdas Tomas Racys, Julian Eastoe, Per-Ola Norrby, Isabelle Grillo, Sarah E. Rogers and Guy C. Lloyd-Jones*

Pd- $\eta^3\text{-C}_6\text{H}_9$ cations bearing the Trost ligand (2) undergo two-stage oligomerisation-aggregation to form high nuclearity aggregates (up to 56 Pd centres), with aggregation strongly modulated by concentration, solvent and counter-anion.

5802

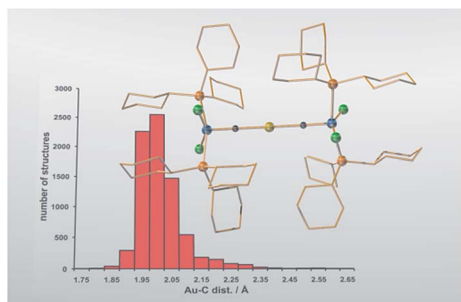


Rh/Rh^{III} catalyst-controlled divergent aryl/heteroaryl C-H bond functionalization of picolinamides with alkynes

Ángel Manu Martínez, Javier Echavarren, Inés Alonso, Nuria Rodríguez,* Ramón Gómez Arrayás* and Juan C. Carretero*

Switchable site-selectivity through catalyst control is achieved in the direct functionalization of picolinamides that contain two distinct C-H sites to construct diverse scaffolds from the same starting material.

5815

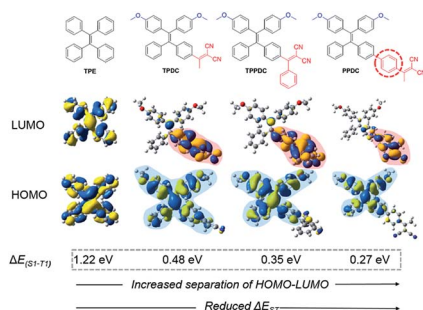


Carbide complexes as π -acceptor ligands

Anders Reinholdt, Johan E. Vibenholt, Thorbjørn J. Morsing, Magnus Schau-Magnussen, Nini E. A. Reeler and Jesper Bendix*

A terminal carbide complex binds as a π -acceptor towards electron-rich metal centers, mirroring CO, and provides the first homoleptic, carbide-ligated complex.

5824



Tuning the singlet-triplet energy gap: a unique approach to efficient photosensitizers with aggregation-induced emission (AIE) characteristics

Shidang Xu, Youyong Yuan, Xiaolei Cai, Chong-Jing Zhang, Fang Hu, Jing Liang, Guanxin Zhang, Deqing Zhang and Bin Liu*

The efficiency of the intersystem crossing process can be improved by reducing the energy gap between the singlet and triplet excited states (ΔE_{ST}), which offers the opportunity to improve the yield of the triplet excited state.

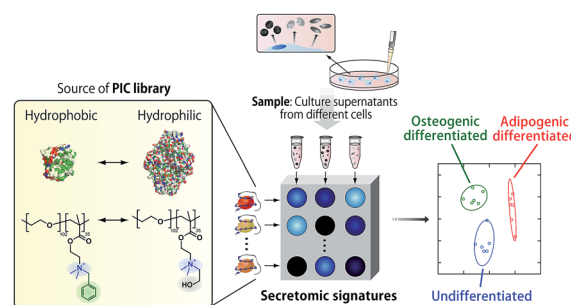


5831

A polyion complex sensor array for markerless and noninvasive identification of differentiated mesenchymal stem cells from human adipose tissue

Shunsuke Tomita,* Miho Sakao, Ryoji Kurita, Osamu Niwa and Keitaro Yoshimoto*

A sensor array of cross-reactive polyion complexes enabled markerless and noninvasive identification of osteogenic and adipogenic differentiation of human mesenchymal stem cells.

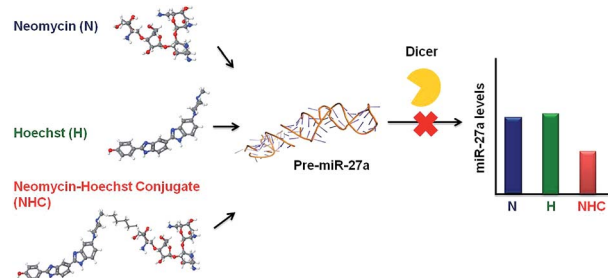


5837

Potent inhibition of miR-27a by neomycin-bisbenzimidazole conjugates

Smita Nahar, Nihar Ranjan, Arjun Ray, Dev P. Arya* and Souvik Maiti*

Potent downregulation of oncogenic miRNA is obtained by conjugation of neomycin and bisbenzimidazoles.

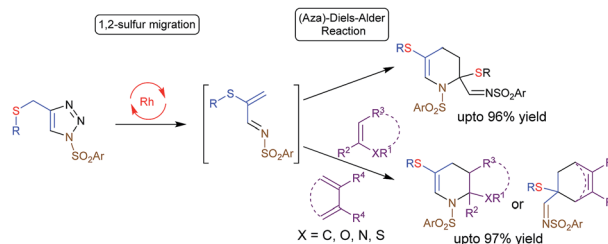


5847

Tandem 1,2-sulfur migration and (aza)-Diels-Alder reaction of β -thio- α -diazoimines: rhodium catalyzed synthesis of (fused)-polyhydropyridines, and cyclohexenes

Dongari Yadagiri and Pazhamalai Anbarasan*

Rhodium catalyzed synthesis of substituted tetrahydropyridines was accomplished from readily accessible thio-tethered *N*-sulfonyl-1,2,3-triazoles.

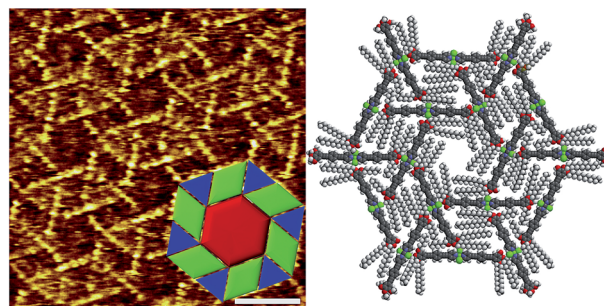


5853

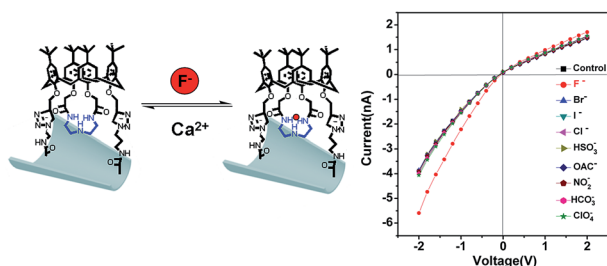
Concentration-dependent rhombitrihexagonal tiling patterns at the liquid/solid interface

Vladimir Stepanenko, Ramesh Kandanelli, Shinobu Uemura, Frank Würthner* and Gustavo Fernández*

A self-assembling Pd(II) complex forms sophisticated concentration-dependent Archimedean tiling patterns composed of three types of polygons at the liquid/solid interface.



5859

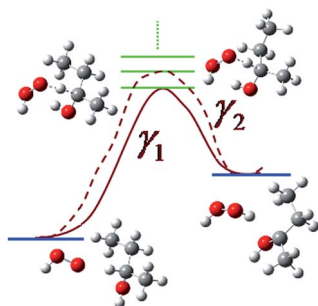


Fluoride responsive single nanochannel: click fabrication and highly selective sensing in aqueous solution

Guanrong Nie, Yue Sun, Fan Zhang, Miaomiao Song, Demei Tian, Lei Jiang and Haibing Li*

A F^- responsive nanochannel based on hydrogen-bonding interactions was designed to accomplish highly selective sensing in aqueous solution.

5866

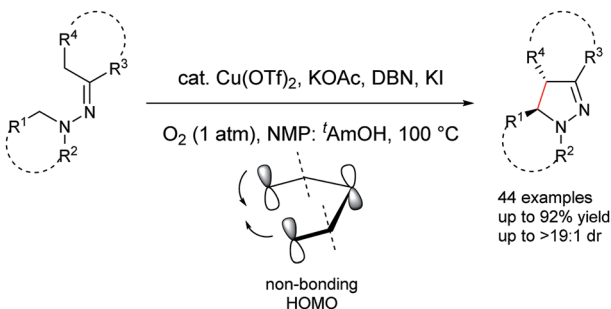


Multi-path variational transition state theory for chiral molecules: the site-dependent kinetics for abstraction of hydrogen from 2-butanol by hydroperoxyl radical, analysis of hydrogen bonding in the transition state, and dramatic temperature dependence of the activation energy

Junwei Lucas Bao, Rubén Meana-Pañeda and Donald G. Truhlar*

A hydrogen bond at the transition state can lower the enthalpy of activation, but raise the free energy of activation.

5882

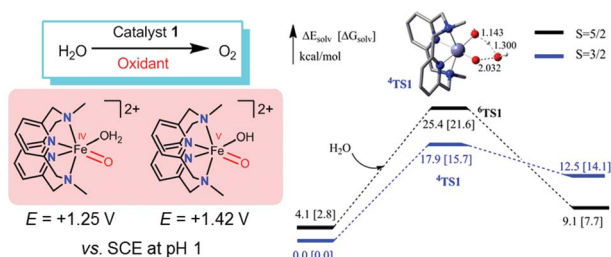


Copper-catalyzed diastereoselective aerobic intramolecular dehydrogenative coupling of hydrazones via sp^3 C–H functionalization

Xuesong Wu, Mian Wang, Guangwu Zhang, Yan Zhao, Jianyi Wang* and Haibo Ge*

Diastereoselective aerobic dehydrogenative cyclization of hydrazones is described via a copper-catalyzed sp^3 C–H functionalization process.

5891



Water oxidation catalysed by iron complex of *N,N'*-dimethyl-2,11-diaza[3,3](2,6)pyridinophane. Spectroscopy of iron–oxo intermediates and density functional theory calculations

Wai-Pong To, Toby Wai-Shan Chow, Chun-Wai Tse, Xiangguo Guan,* Jie-Sheng Huang and Chi-Ming Che*

$Fe^{IV}=O$ and/or $Fe^V=O$ intermediates are suggested to be involved in water oxidation with $[NH_4]_2[Ce^{IV}(NO_3)_6]$, $NaIO_4$, or Oxone catalyzed by $[Fe^{III}(L1)Cl_2]^+$ (1) on the basis of spectroscopic measurements and DFT calculations.

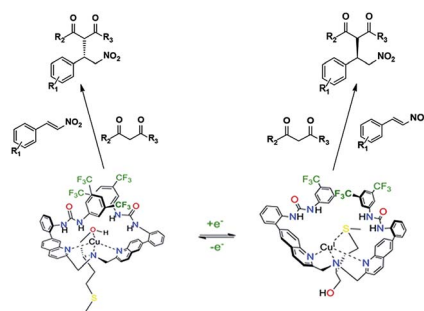


5904

Redox-configurable ambidextrous catalysis: structural and mechanistic insight

Shahab Mortezaei, Noelle R. Catarineu, Xueyou Duan, Chunhua Hu and James W. Canary*

A helically chiral copper complex is used as a switchable asymmetric catalyst capable of delivering either enantiomer of a Michael addition reaction.

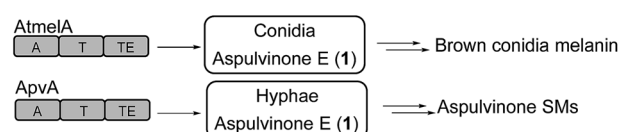


5913

Spatial regulation of a common precursor from two distinct genes generates metabolite diversity

Chun-Jun Guo, Wei-Wen Sun, Kenneth S. Bruno, Berl R. Oakley, Nancy P. Keller and Clay C. C. Wang*

We have demonstrated that spatial regulation of the same product from two distinct genes generates metabolite diversity.

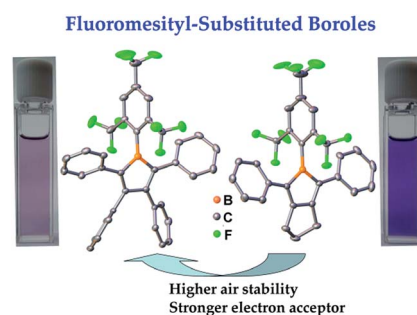


5922

Taming the beast: fluoromesityl groups induce a dramatic stability enhancement in boroles

Zuolun Zhang, Robert M. Edkins, Martin Haehnel, Marius Wehner, Antonius Eichhorn, Lisa Mailänder, Michael Meier, Johannes Brand, Franziska Brede, Klaus Müller-Buschbaum, Holger Braunschweig and Todd B. Marder*

Boroles with a fluoromesityl group on the B atom have greatly improved air stability compared to their mesityl analogues.

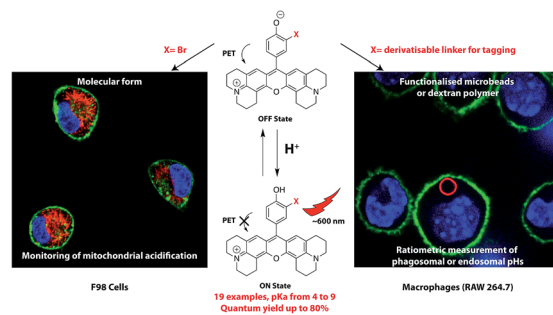


5928

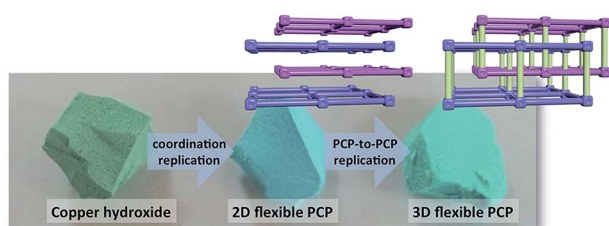
H-Rubies, a new family of red emitting fluorescent pH sensors for living cells

Guillaume Despras, Alsu I. Zamaleeva, Lucie Dardevet, Céline Tisseyre, Joao Gamelas Magalhaes, Charlotte Garner, Michel De Waard, Sebastian Amigorena, Anne Feltz, Jean-Maurice Mallet and Mayeul Collot*

H-Rubies is a family of pH probes that display a bright red fluorescence upon acidification. They have been used as molecular form to monitor mitochondrial acidification and as functionalised forms to provide ratiometric systems to measure phagosomal and endosomal pH in macrophages.



5938

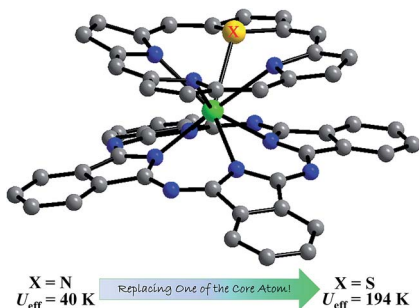


Mesoscopic superstructures of flexible porous coordination polymers synthesized *via* coordination replication

Kenji Sumida, Nirmalya Moitra, Julien Reboul, Shotaro Fukumoto, Kazuki Nakanishi, Kazuyoshi Kanamori, Shuhei Furukawa* and Susumu Kitagawa*

Monolithic superstructures of two- and three-dimensional flexible frameworks are prepared *via* coordination replication from a copper hydroxide parent phase.

5947

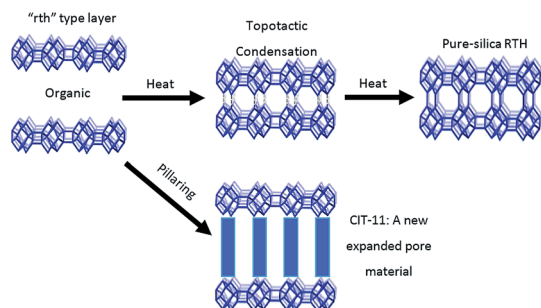


Rational enhancement of the energy barrier of bis(tetrapyrrole) dysprosium SMMs *via* replacing atom of porphyrin core

Wei Cao, Chen Gao, Yi-Quan Zhang, Dongdong Qi, Tao Liu,* Kang Wang, Chunying Duan, Song Gao* and Jianzhuang Jiang*

Replacing a porphyrin N atom induces higher electrostatic environment anisotropy around the Dy center, giving the highest energy barrier among bis(tetrapyrrole) Dy SMMs.

5955

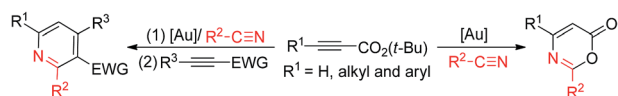


Synthesis of the RTH-type layer: the first small-pore, two dimensional layered zeolite precursor

Joel E. Schmidt, Dan Xie and Mark E. Davis*

The "rth" type layer is the first porous 2D zeolite layer; it forms zeolite RTH *via* topotactic condensation or can be pillared to create a thermally stable, expanded pore material.

5964



Gold-catalyzed formal $[4\pi + 2\pi]$ -cycloadditions of propiolate derivatives with unactivated nitriles

Somnath Narayan Karad, Wei-Kang Chung and Rai-Shung Liu*

Gold-catalyzed hetero- $[4\pi + 2\pi]$ -cycloadditions of *tert*-butyl propiolates with unactivated nitriles are described. This new finding enables a one-pot gold-catalyzed synthesis of highly substituted pyridines.

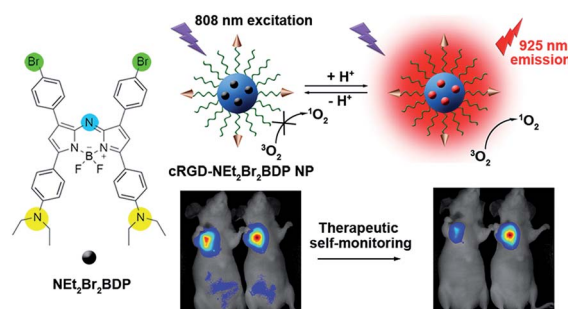


5969

A pH-activatable and aniline-substituted photosensitizer for near-infrared cancer theranostics

Jiangwei Tian, Jinfeng Zhou, Zhen Shen, Lin Ding, Jun-Sheng Yu and Huangxian Ju*

A trifunctional photosensitizer was designed to achieve highly selective near-infrared tumor imaging, efficient photodynamic therapy and therapeutic self-monitoring.



5978

Pyridine-enabled copper-promoted cross dehydrogenative coupling of C(sp²)–H and unactivated C(sp³)–H bonds

Xuesong Wu, Yan Zhao and Haibo Ge*

Pyridine-enabled cross dehydrogenative coupling of sp² C–H bonds of polyfluoroarenes and unactivated sp³ C–H bonds of amides was achieved.

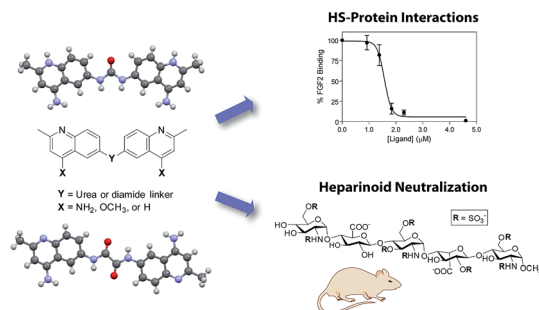


5984

Small molecule antagonists of cell-surface heparan sulfate and heparin–protein interactions

Ryan J. Weiss, Philip L. S. M. Gordts, Dzung Le, Ding Xu, Jeffrey D. Esko and Yitzhak Tor*

A series of rationally designed surfen analogs were synthesized and utilized as antagonists of glycosaminoglycan–protein interactions, including the neutralization of the anticoagulant activity of fondaparinux, a synthetic pentasaccharide analog of heparin.

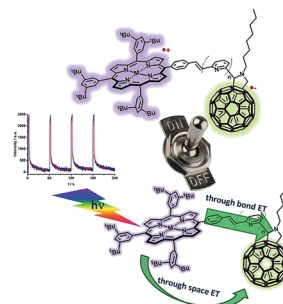


5994

On–off switch of charge-separated states of pyridine–vinylene-linked porphyrin–C₆₀ conjugates detected by EPR

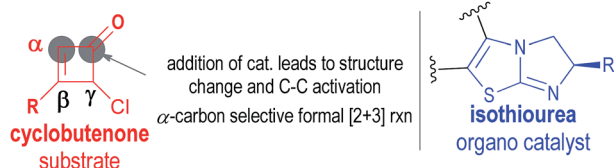
S. V. Kirner, D. Arteaga, C. Henkel, J. T. Margraf, N. Alegret, K. Ohkubo, B. Insuasty, A. Ortiz,* N. Martin, L. Echegoyen,* S. Fukuzumi,* T. Clark and D. M. Guldi*

The on–off switch of charge separated states in a new series of pyridine–vinylene linked porphyrin–C₆₀ conjugates was detected by EPR at 77 K.



EDGE ARTICLES

6008

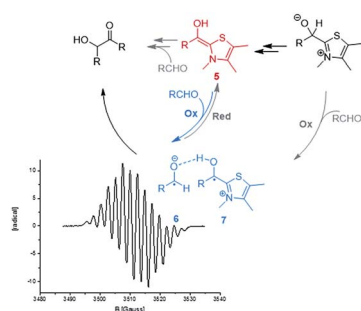


Cycloaddition of cyclobutenone and azomethine imine enabled by chiral isothiourea organic catalysts

Bao-Sheng Li, Yuhuang Wang, Zhichao Jin and Yonggui Robin Chi*

An organocatalytic carbon–carbon bond activation of γ -mono-chlorine substituted cyclobutenone provides an α -carbon selective cycloadduct with excellent stereoselectivities.

6013



NHC-catalysed benzoin condensation – is it all down to the Breslow intermediate?

Julia Rehbein,* Stephanie-M. Ruser and Jenny Phan

The NHC-catalysed benzoin condensation has been studied mechanistically by a combination of experimental and computational chemistry. The presented EPR-spectroscopic and computational data provide evidence for a radical pair as a potential second key-intermediate that is derived from the Breslow-intermediate via an SET process.

CORRECTIONS

6019

Correction: Characterizing chain processes in visible light photoredox catalysis

Megan A. Cismesia and Tehshik P. Yoon*

6020

Correction: Fluorescent carbon dot–molecular salt hydrogels

Angelina Cayuela, Stuart R. Kennedy, M. Laura Soriano, Christopher D. Jones, Miguel Valcárcel* and Jonathan W. Steed*



CORRECTIONS

6021

Correction: Humidity-dependent surface tension measurements of individual inorganic and organic submicrometre liquid particles

Holly S. Morris, Vicki H. Grassian* and Alexei V. Tivanski*

